Supplement: Testing the Pattern of AKT Activation by Variational Parameter Estimation

Daniel Kaschek, Frauke Henjes, Max Hasmann, Ulrike Korf and Jens Timmer

I. Model equations

The mTOR signaling pathway model is composed of 21 elementary reactions, presented in the following overview where each reaction, first column, occurs with a specific rate, second column. A short description of the process is appended in third column.

	Reaction	Rate	Description
1	R2 -> pR2	actR2*R2	Basal phosphorylation of ERBB2
2	pR2 -> R2	deactpR2*pR2	Basal de-phosphorylation of ERBB2
3	R2 -> pR2HRG	actR2ByHRG*R2*HRG	HRG induced formation of phosphorylated ERBB2-ERBB3 dimers
4	pR2 -> pR2HRG	actpR2ByHRG*pR2*HRG	HRG induced formation of phosphorylated ERBB2-ERBB3 dimers
5	pR2HRG ->	degpR2HRG*pR2HRG	Basal degradation of ERBB2-ERBB3 dimers
6	pR2HRG -> R2	deactpR2HRGtyr*pTAkt*pR2HRG	Degradation of ERBB2-ERBB3 dimers related to threonine phosphorylation
7	pR2HRG -> R2	deactpR2HRGser*pSAkt*pR2HRG	Degradation of ERBB2-ERBB3 dimers related to serine phosphorylation
8	pR2HRG -> R2	deactpR2HRGtyr*pSpTAkt*pR2HRG	Degradation of ERBB2-ERBB3 dimers related to threonine phosphorylation
9	pR2HRG -> R2	deactpR2HRGser*pSpTAkt*pR2HRG	Degradation of ERBB2-ERBB3 dimers related to serine phosphorylation
10	Akt -> pSAkt	actSirAktBase*Akt*mTOR	mTOR-induced serine phosphorylation
11	Akt -> pSAkt	actSirAktBase0*Akt	Basal serine phosphorylation
12	pSAkt -> Akt	deactpSAktBase*pSAkt	Basal de-phosphorylation of pS-Akt
13	Akt -> pTAkt	actTyrAktBase*Akt*pR2HRG	Receptor-induced threonine phosphorylation
14	Akt -> pTAkt	actTyrAktBase0*Akt	Basal threonine phosphorylation
15	pTAkt -> Akt	deactpTAktBase*pTAkt	Basal de-phosphorylation of pT-Akt
16	pTAkt -> pSpTAkt	actSirAkt*pTAkt*mTOR	mTOR-induced serine phosphorylation
17	pTAkt -> pSpTAkt	actSirAktSeq*pTAkt*mTOR	mTOR-induced serine phosphorylation
18	pSpTAkt -> pTAkt	deactpSAkt*pSpTAkt	Basal de-phosphorylation of pSpT-Akt
19	pSAkt -> pSpTAkt	actTyrAkt*pSAkt*pR2HRG	Receptor-induced threonine phosphorylation

```
20   pSAkt  ->   pSpTAkt            actTyrAktSeq*pSAkt  Basal threonine
                                                        phosphorylation
21   pSpTAkt  ->   pSAkt            deactpTAkt*pSpTAkt  Basal de-phosphorylation
                                                        of pSpT-Akt
```

The elementary reactions are combined into one ODE collecting the loss and the gain terms for each reactant. Since the variational input estimation method as being employed in this study requires that observables correspond to states of the ODE, a variable transformation is performed. The transformation and the corresponding inverse transformation read:

```
Transformation of variables       Inverse transformation
y1 = pR2 + pR2HRG                 pR2     = y1 - y5
y2 = pSAkt + pSpTAkt              pR2HRG  = y5
y3 = (pTAkt + pSpTAkt)/s3         pSAkt   = y2 - y7
y4 = R2                           pTAkt   = s3*y3 - y7
y5 = pR2HRG                       pSpTAkt = y7
y6 = Akt                          R2      = y4
y7 = pSpTAkt                      AKT     = y6
```

The ODE expressed in the new variables is

```
d/dt y1 = HRG*actR2ByHRG*y4 + actR2*y4 - deactpR2*(y1 - y5) - deactpR2HRGser*y5*y7 +
          -deactpR2HRGser*y5*(y2 - y7) - deactpR2HRGtyr*y5*y7 +
          -deactpR2HRGtyr*y5*(s3*y3 - y7) - degpR2HRG*y5
d/dt y2 = actSirAkt*mTOR*(s3*y3 - y7) + actSirAktBase*mTOR*y6 + actSirAktBase0*y6 +
          +actSirAktSeq*mTOR*(s3*y3 - y7) - deactpSAkt*y7 - deactpSAktBase*(y2 - y7)
d/dt y3 = actTyrAkt*y5*(y2 - y7)/s3 + actTyrAktBase*y5*y6/s3 + actTyrAktBase0*y6/s3 +
          +actTyrAktSeq*(y2 - y7)/s3 - deactpTAkt*y7/s3 - deactpTAktBase*(s3*y3 - y7)/s3
d/dt y4 = -HRG*actR2ByHRG*y4 - actR2*y4 + deactpR2*(y1 - y5) + deactpR2HRGser*y5*y7 +
          +deactpR2HRGser*y5*(y2 - y7) + deactpR2HRGtyr*y5*y7 +
          +deactpR2HRGtyr*y5*(s3*y3 - y7)
d/dt y5 = HRG*actR2ByHRG*y4 + HRG*actpR2ByHRG*(y1 - y5) - deactpR2HRGser*y5*y7 +
          -deactpR2HRGser*y5*(y2 - y7) - deactpR2HRGtyr*y5*y7 +
          -deactpR2HRGtyr*y5*(s3*y3 - y7) - degpR2HRG*y5
d/dt y6 = -actSirAktBase*mTOR*y6 - actSirAktBase0*y6 - actTyrAktBase*y5*y6 +
          -actTyrAktBase0*y6 + deactpSAktBase*(y2 - y7) + deactpTAktBase*(s3*y3 - y7)
d/dt y7 = actSirAkt*mTOR*(s3*y3 - y7) + actSirAktSeq*mTOR*(s3*y3 - y7) +
          +actTyrAkt*y5*(y2 - y7) + actTyrAktSeq*(y2 - y7) - deactpSAkt*y7 +
          -deactpTAkt*y7
```

where the states `y1, y2` and `y3` describe the observed ERBB2 phosphorylation, AKT serine phosphorylation and AKT threonine phosphorylation.

The mTOR input is connected to the adjoint equations via

```
mTOR = (mTORD - ((actSirAkt*(s3*y3-y7)+actSirAktBase*y6+actSirAktSeq*(s3*y3-y7)) *
       adjy2 + (-(actSirAktBase*y6)) * adjy6 +
       (actSirAkt*(s3*y3-y7)+actSirAktSeq*(s3*y3-y7)) * adjy7/weightmTORD)
```

II. Parameter transformations

The two model hypotheses are implemented by fixing rate parameters and initial conditions. Furthermore, initial value parameters are expressed by the corresponding steady state conditions:

```
Activation path 1:
actTyrAktBase  = 0
actTyrAktBase0 = 0
deactpTAktBase = 0
actSirAkt      = 0
actSirAktSeq   = 0
deactpSAkt     = 0
y5             = 0
y1             = actR2SS*y4/deactpR2SS
```

```
y2              = ((actSirAktBase0+actSirAktBaseSS*mTOR0)/deactpSAktBase)*
                  *(1+actTyrAktSeq/deactpTAkt)*y6
y7              = ((actSirAktBase0+actSirAktBaseSS*mTOR0)/deactpSAktBase)*
                  *(actTyrAktSeq/deactpTAkt)*y6
y3              = y7/s3

Activation path 2:
actSirAktBase  = 0
actSirAktBase0 = 0
deactpSAktBase = 0
actTyrAkt      = 0
actTyrAktSeq   = 0
deactpTAkt     = 0
y5              = 0
y1              = actR2SS*y4/deactpR2SS
y3              = ((actTyrAktBase0)/deactpTAktBase)*
                  *(1+(actSirAktSeqSS+actSirAktSS*mTOR0)/deactpSAkt)*y6/s3
y7              = ((actTyrAktBase0)/deactpTAktBase)*
                  *((actSirAktSeqSS+actSirAktSS*mTOR0)/deactpSAkt)*y6
y2              = y7
```

In addition to these "global" parameter transformations, i.e. the parameter expressions are valid for all experimental conditions, some of the parameters are individualized for each condition. The following parameters are allowed to take different values for each experimental condition:

```
actSirAktBase, actR2, deactpR2, actR2ByHRG, actpR2ByHRG, degpR2HRG
```

Finally, all parameters were fitted logarithmically, i.e. the global parameter transformation $p \longrightarrow logp = \ln(p)$ was performed.

III. Random initialization

In non-linear optimization problems typically several local optima exist. Therefore, the solution of the optimization problem may depend on the initialization of the parameter values. To increase the chance of finding the best optimum, optimization was run from different initial positions. Here, 500 initial parameters were randomly drawn from a normal distribution around $\mu = \ln(0.1)$ with standard deviation $\sigma = 1$. Fig. 1 shows the objective values after optimization for the two model hypotheses.

IV. Observability

One complication of parameter estimation in partially observed systems is non-observability: trajectories of the unobserved states can be highly variable although they coincide for the observed states. One possibility to check observability is by multiple fitting from differently initialized parameter values. In case, the system is non-observable, different fits with the same final objective value can exhibit differing trajectories of the unobserved states. Figs. 2 and 3 show the trajectories corresponding to the 100 best fits for both model hypotheses. In general, both model hypotheses show good observability. For hypothesis 1, Fig. 2, pSpT-AKT has the largest uncertainty: all green curves have slightly different pSpT-AKT levels. Similarly, the blue curves which correspond to a different local optimum show a large variance for pSpT-AKT, but also ERBB2. In case of hypothesis 2, the best fits in red have different ERBB2 levels. The same holds for the green curves corresponding to a different local optimum as can be seen from the pERBB2 and pERBB2•HRG trajectories.

Different local optima are not only characterized by different trajectories but by different objective values, too. Although Fig. 1b indicates several jumps of the sorted objective values, those values corresponding to the same optimum do not exhibit the exact same value. This can have at least two reasons:

1) The precision by which the adjoint sensitivities are computed is limited.[1] Accordingly, the gradient derived from the sensitivities is misspecified, leading to premature termination of the optimization run.
2) The approximation of the Hessian matrix by the SR1 update formula might be insufficient to guarantee full convergence.

These issues can present a considerable drawback, especially when the exact optimal parameter values are the major target. In contrast, when focusing on the prediction of unobserved states, the differences in final objective values can be of minor importance for the accuracy of the predicted time courses as being the case for our study, see Figs. 2 and 3.

[1] See e.g. Bryson, Arthur Earl. *Applied Optimal Control: Optimization, Estimation and Control*. CRC Press, 1975.

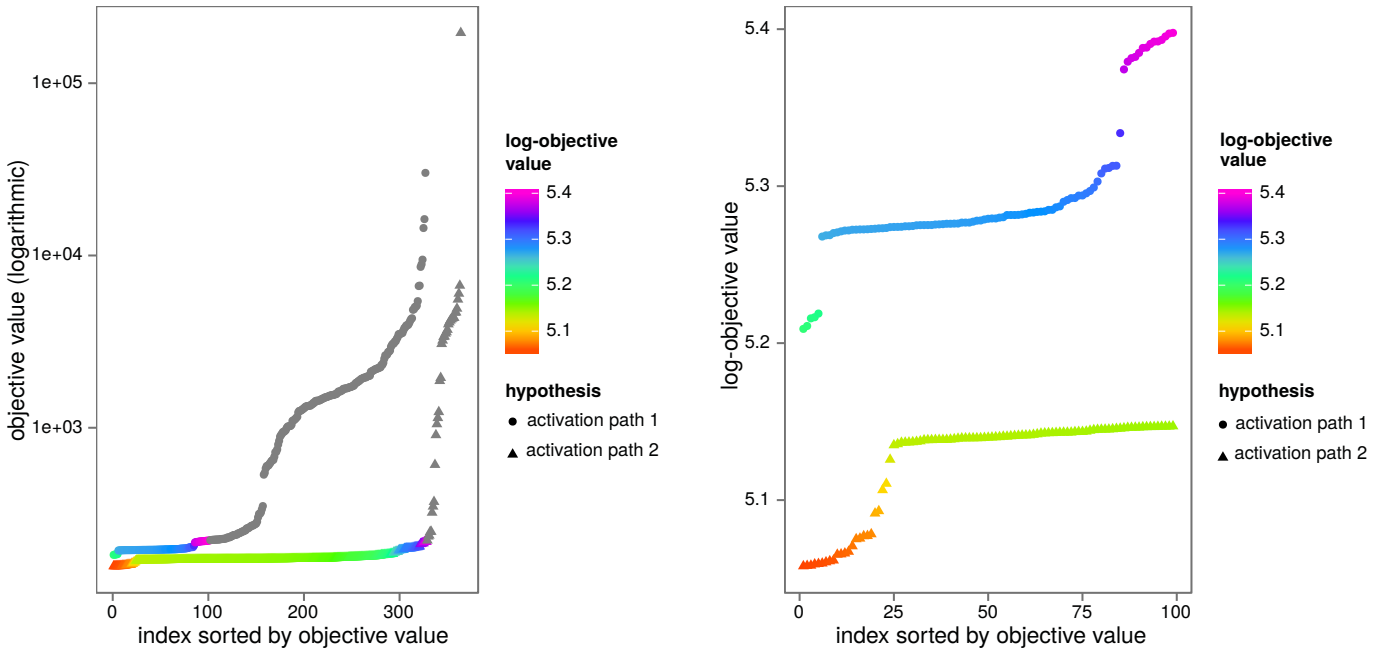

(a) All fits

(b) Best 100 fits

Fig. 1: Sorted objective values for the two model hypotheses after optimization. Different hypotheses are indicated by different symbols. Colors correspond to different objective values after parameter optimization between $5.05 = \ln(156)$ and $5.4 = \ln(221)$. The fits per hypothesis have been sorted according to their objective value, indicated as index.

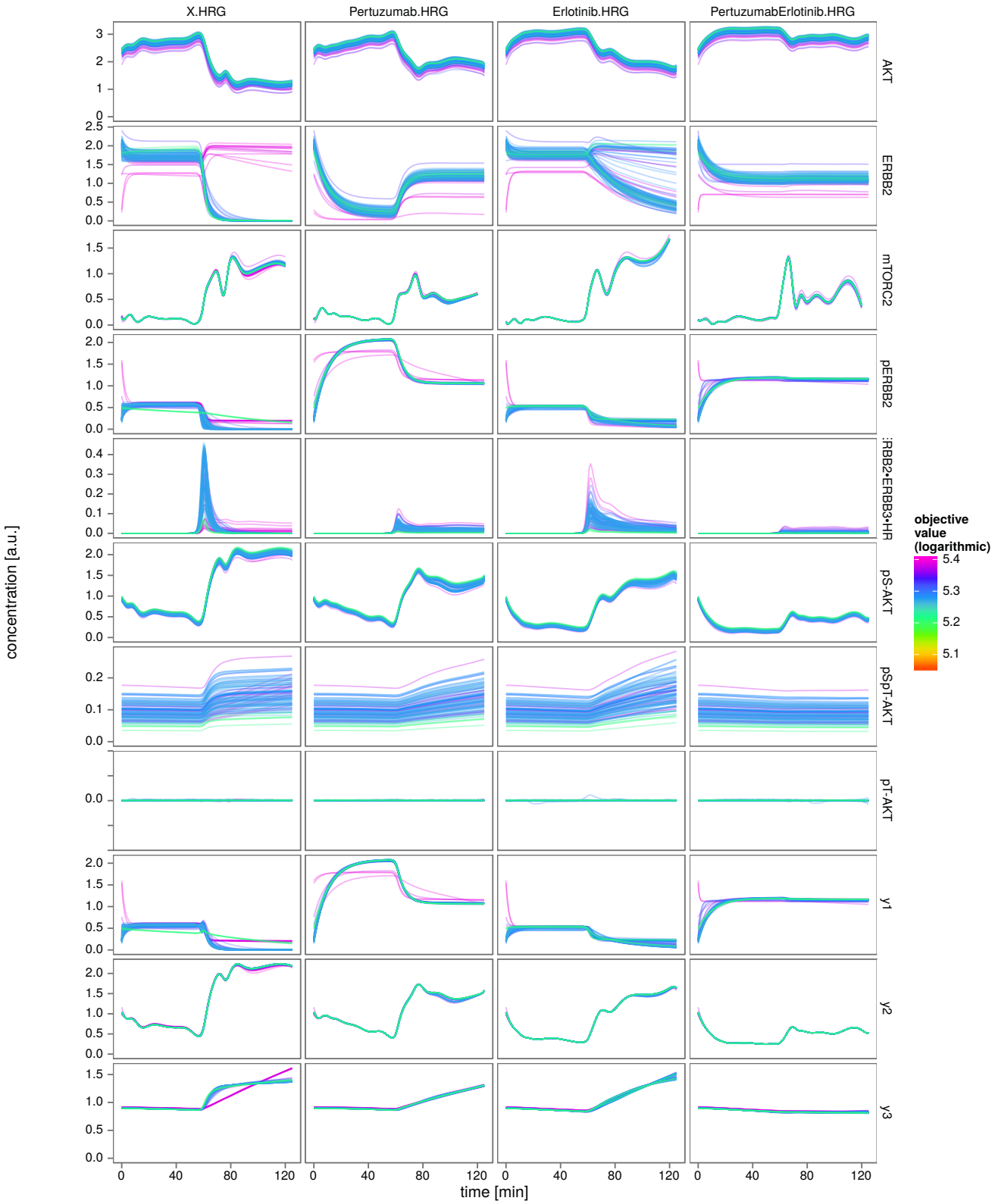

Fig. 2: Trajectories of model hypothesis 1. The trajectories for the 100 best fits are plotted in different colors according to their objective value. The columns correspond to experimental conditions, rows correspond to different targets.

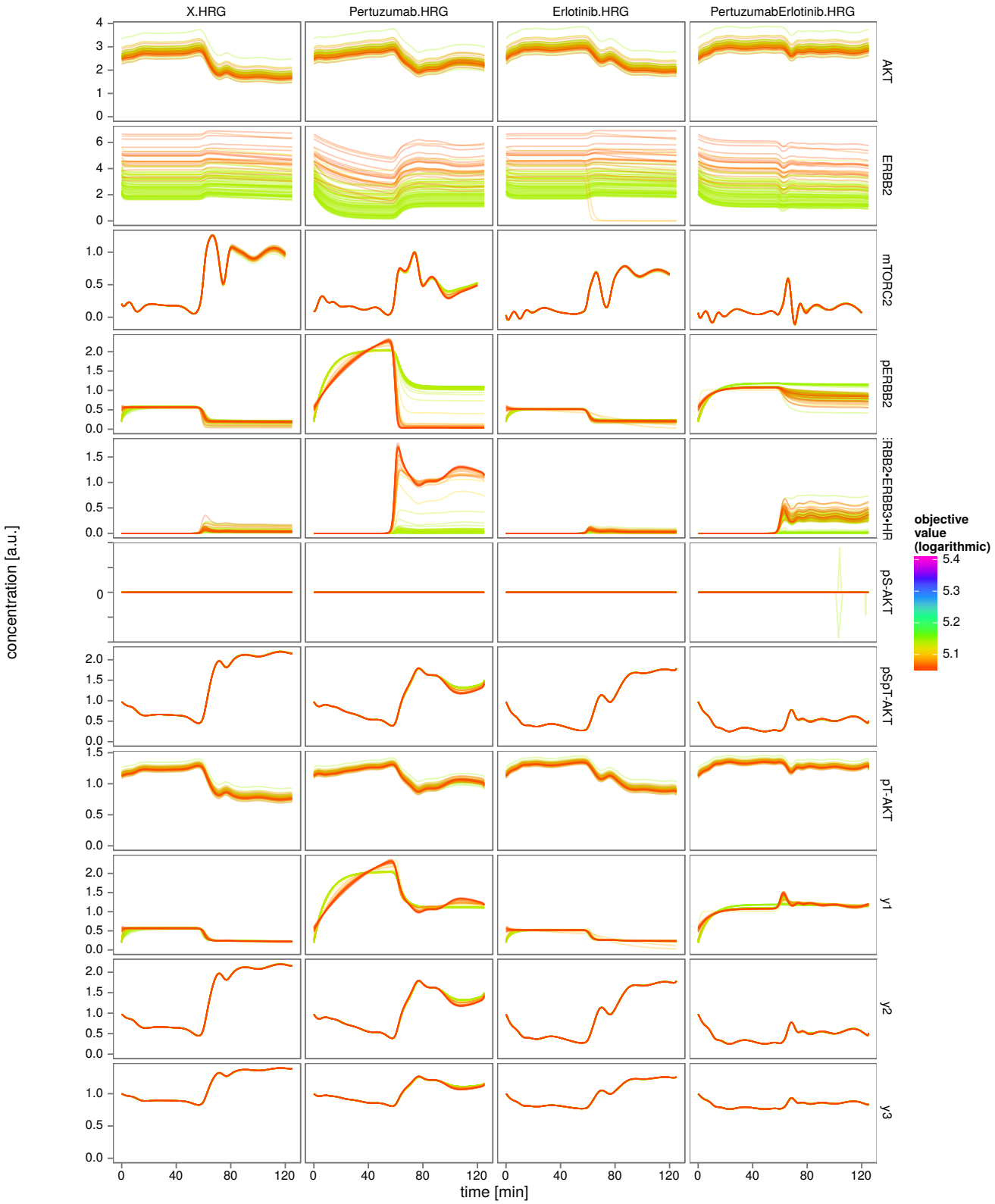

Fig. 3: Trajectories of model hypothesis 2. The trajectories for the 100 best fits are plotted in different colors according to their objective value. The columns correspond to experimental conditions, rows correspond to different targets.